International Journal of Heat and Mass Transfer 85 (2015) 311–320

Contents lists available at ScienceDirect

International Journal of Heat and Mass Transfer

journal homepage: www.elsevier.com/locate/ijhmt

Radiative heating of superficial human tissues with the use of water-filtered infrared-A radiation: A computational modeling

Leonid A. Dombrovsky [a,*], Victoria Timchenko [b], Chinmay Pathak [b], Helmut Piazena [c], Werner Müller [d], Michael Jackson [e]

[a] Joint Institute for High Temperatures, Krasnokazarmennaya 17A, NCHMT, Moscow 111116, Russia
[b] School of Mechanical and Manufacturing Engineering, University of New South Wales, Sydney 2052, Australia
[c] Medical Photobiology Group, Charité – Universitätsmedizin Berlin, Berlin, Germany
[d] Dr. h.c. Erwin Braun Foundation Basel, Switzerland
[e] Prince of Wales Clinical School, University of New South Wales, Sydney 2052, Australia

ARTICLE INFO

Article history:
Received 28 October 2014
Received in revised form 20 January 2015
Accepted 29 January 2015

Keywords:
Hyperthermia
Infrared radiation
Radiative transfer
Spectral calculations
Transient heat transfer
Computational model

ABSTRACT

A computational model of both the absorbed radiation and transient temperature fields in multilayer superficial human tissues in the case of an external water-filtered infrared-A irradiation is developed. A novel simplified model for radiative transfer is based on local 1-D solutions taking into account the oblique incidence of radiation at the periphery of the heated region. The computational study of a model problem at typical geometrical, optical, and thermal parameters confirms the acceptable accuracy of the 1-D solution for the temperature field formed in human tissues during thermal treatment with periodic infrared irradiation. The effects of uncertainties in spectral absorption coefficients and thermal conductivity of biological tissues on thermal treatment parameters are analyzed. It is shown that the temperature response to periodic water-filtered infrared-A heating can be used to estimate optical properties of human tissues. The calculations show that the decrease in convective heat transfer with the heating of air in the gap between the radiation source and the body surface has to be taken into account.

1. Introduction

In clinical applications, water-filtered infrared-A (wIRA) irradiation is generated by passing the full spectrum of radiation of a halogen bulb through a cuvette, containing water, to reduce the undesired irradiation within the spectral range characterized by high values of the absorption coefficient of water. After water filtering, the spectrum of the transmitted radiation is within the therapeutically desired window ($0.78 < \lambda < 1.4$ μm) and therefore can produce a therapeutically usable volumetric heating of the tissue. In addition, the ability of wIRA to penetrate deeply into tissues stimulates the basic energy processes in the mitochondria of cells within the exposed area and results in direct stimuli on cells and cellular structures [1].

Due to the increase of the tissue temperature as well as the improvement of both the energy supply per time (increase of metabolic rate) and the oxygen supply, wIRA has shown good clinical effects on wounds and wound infections [2] as well as in applications of photodynamic therapy [3]. Thermography guided water-filtered infrared-A hyperthermia has been successfully used for local recurrent breast cancer with promising clinical results [4].

Despite the various applications of wIRA irradiation in medicine the methodological description in studies of cellular responses after wIRA exposure in single cells and skin is insufficient or absent [5]. This includes information about the experimental setups for wIRA exposure (e.g., wIRA emitter, water filter thickness, other filter sets, the resulting spectral irradiance of the unit); the method of cooling or temperature regulation of the sample during irradiation (i.e., air or water cooling, temperature measurement of the sample); environmental conditions; room temperature and humidity; the absorption spectra of the media used and cell culture materials; or the thermography employed in the experimental setup. In addition, computational modeling of wIRA applied to hyperthermia of superficial tumors has been very limited.

Therefore, in this paper we focus on the development of a model for radiative heating of superficial human tissues with the use of water-filtered infrared-A radiation. At the first step of modeling, the normal (healthy) skin tissues are considered. There are two methodological differences in modeling of wIRA irradiation as compared with the models developed in previous studies of laser-induced hyperthermia [6–11]:

* Corresponding author. Tel.: +7 499 250 3264; fax: +7 495 362 5590.
E-mail address: ldombr@yandex.ru (L.A. Dombrovsky).

http://dx.doi.org/10.1016/j.ijheatmasstransfer.2015.01.133
0017-9310/

Nomenclature

c	specific heat capacity
d	thickness of the computational region for radiative transfer calculations
D	radiation diffusion coefficient
E	function introduced by Eq. (8)
f	function introduced by Eq. (23)
F, G	functions introduced by Eq. (9a)
g	unknown function in Eq. (12a)
h	heat transfer coefficient
H	distance from the light source to the body surface
I	radiation intensity
J	diffuse radiation intensity
k	thermal conductivity
L	thickness of the computational region for heat transfer calculations
n	index of refraction
q	radiative flux
$\vec{r}$	spatial coordinate
r	radial coordinate
R	reflectance, radius of the region
w, W	absorbed radiation power
z	axial coordinate

Greek symbols

α	absorption coefficient
β	extinction coefficient
γ	coefficient introduced by Eq. (12c)
θ	angle measured from the normal
κ	index of absorption
λ	wavelength
μ	cosine of an angle
$\bar{\mu}$	asymmetry factor of scattering
ρ	density
σ	scattering coefficient
τ	optical thickness
$J^{\mp}, J^{0}$	functions introduced by Eq. (11)
ω	scattering albedo
$\vec{\Omega}$	unit vector of direction

Subscripts and superscripts

cr	critical
e	ext external
f	Fresnel's
h	heating
i	incident
int	internal
n	normal
s	surface
tr	transport
λ	spectral

- The incident radiation is not monochromatic;
- The incident radiation is not collimated, and there are various angular distributions of the radiation intensity at different points of the illuminated area (see Fig. 1).

The first of the above special features of the problem under consideration requires spectral data for all the tissues and increases the computational time. Therefore, the use of an approximate solution for radiative transfer at every wavelength is important to avoid time-consuming calculations.

The complex angular dependence of the incident radiation makes the use of traditional approximations which are developed for totally diffuse or collimated irradiation problematic. In this paper, a novel simplified approach based on the modified two-flux approximation for 1-D problem at oblique incidence is suggested. For simplicity, average angles of incidence are considered at each of several thin concentric layers of the axisymmetric computational region.

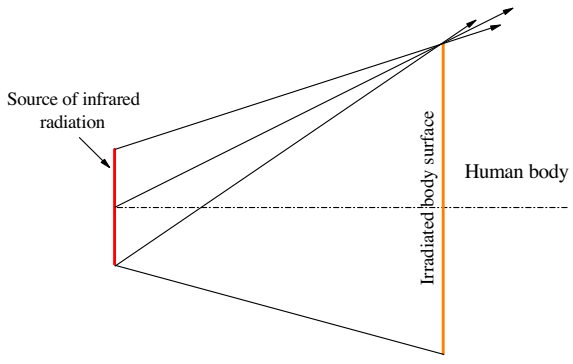

Fig. 1. Scheme of irradiation of the body surface in wIRA method.

A complete 2-D problem statement is employed to solve the transient heat transfer problem with a volumetric heat source generated mainly from the absorbed power of the external infrared radiation.

The objective of the present paper is two-fold: (1) to develop and examine an approximate method for calculating the absorbed radiation power in the case of a non-collimated near-infrared external radiation at oblique incidence and to examine the applicability of a simplified approach based on the model of local normal incidence; (2) to solve a model transient heat transfer problem at parameters close to the realistic ones for the case of a wIRA thermal treatment of superficial tissues. The applicability of the 1-D approach for the heat transfer calculation is also examined.

2. Spectral optical properties of superficial tissues

Human skin is composed of three main layers, the epidermis, dermis and subcutaneous adipose layer, or subcutaneous fat. The epidermis, which is the outermost layer, is approximately 100 μm thick and contains no blood vessels. The dermis, which is the layer just below the epidermis, can be between 1 and 4 mm thick and is the vascularised layer (contains blood vessels). Below the epidermis lies the subcutaneous fat layer, which can be between 1 and 6 mm thick and serves the purpose of attaching the upper layers of skin to the underlying bone and muscle while supplying blood vessels and nerves [12]. As a result, human skin presents a complex heterogeneous medium and the difference in optical properties of each of these layers in the wavelength range of wIRA irradiation has to be considered.

All subsequent calculations were performed by using data of spectral irradiance of the commonly used wIRA radiator, type *Hydrosun 750* (775 W, Hydrosun GmbH, Müllheim, Germany) which was equipped with filter type *BTE 595*. Spectral irradiance data shown in Fig. 2 were measured at the geometric center of

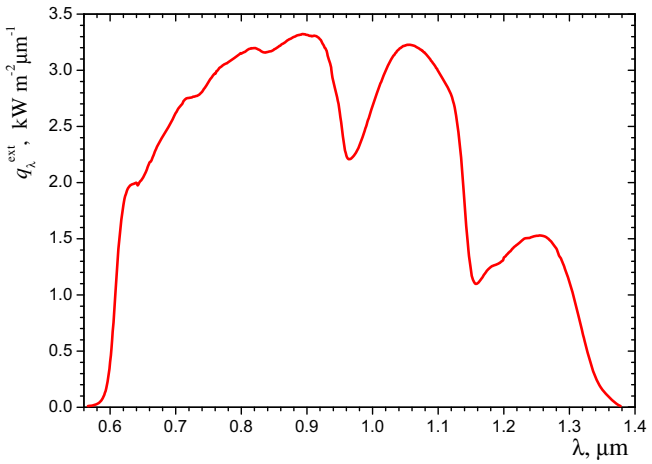

Fig. 2. Spectral radiative flux at the center of the irradiated area.

the exposed area by using a double monochromator radiometer (type *Spectro 320 D*, Instrument Systems, Munich, Germany) equipped with an Ulbricht sphere as optical head. The measurement was taken at a distance of 34 cm between the area of incidence and the exit window of the radiator, which is the recommended distance to the skin for therapeutic applications. Both, the exit window of the radiator and the entrance window of the Unbricht sphere were parallel to each other. According to Fig. 2, the spectrum of the radiator is limited at wavelengths between about $\lambda_1 = 0.566$ μm and about $\lambda_2 = 1.378$ μm. Integration of spectral irradiance data within these limits according to:

$$q^{ext} = \int_{\lambda_1}^{\lambda_2} q_\lambda^{ext}(\lambda) d\lambda \tag{1}$$

results in an incident irradiance of 1728.3 W m^{-2}.

Spectral data for the optical properties of skin tissues can be found in several books and review papers [12–16]. An analysis of the existing experimental data for the main optical properties in the wIRA spectral range shows large discrepancies between optical properties of the skin obtained from various published research, and therefore, a comparative analysis of optical parameters obtained from different experiments has been performed. The analysis was categorized by epidermis, dermis and subcutaneous fat layers in order to compare the optical properties obtained for each layer. A comparison of the optical properties from the early research papers is summarized in Table 1.

In addition, Piazena et al. [5] and Bashkatov et al. [23] presented comparative studies of published results in their respective papers which overlapped with research papers, such as [19,22]. In certain cases there were very slight discrepancies between results presented in the original research paper and those presented in [5,23]. Although these results were expected to be identical, the differences were minor and were attributed to slight errors in the process of extracting results from the original papers.

The absorption coefficients of superficial human tissues presented in Fig. 3a indicate very similar chemical composition of all three superficial tissues. As to Fig. 3b, it is clear that submicron particles of approximately the same size are responsible for scattering in these tissues in the spectral range under consideration [24]. At the same time, the volume fraction of these scattering particles in the epidermis is about twice that in the dermis and fat layers. The uncertainty of the published experimental data for transport scattering coefficients and refraction indices has been found to be insignificant. At the same time, there is a significant difference in absorption coefficients reported by various authors [15–23] for the range of semi-transparency. Therefore, two variants of the absorption coefficient have been considered for dermis as shown in Fig. 3a. The data for the spectral absorption coefficient from [18] were extrapolated to the short-wave range assuming that these values are constant at $\lambda < 0.8$ μm. The data of [18] can be treated as an upper estimate for the absorption coefficient of dermis. For simplicity, the value of index of refraction, n, is assumed constant at 1.45 over the computational region in subsequent calculations.

3. Radiative transfer modeling

The radiative transfer problem under consideration is more complicated than that for collimated irradiation of human body in the normal direction considered in the case of laser-induced hyperthermia [8,9]. The main methodological difficulty is not in the complex spectral composition of the incident infrared radiation but in the complex geometrical characteristics of the external beam. The radiation is not collimated and every point of the body surface is irradiated from different directions because the diameter of the light source (lamp) is comparable with the distance between the light source and the body surface. Moreover, the local average direction of the incident radiation defined using the center of the light source is not normal and depends on the radial distance from the axis of symmetry (see Fig. 1). Strictly speaking, the 1-D radiative transfer model recommended in paper [10] is not directly applicable to this problem.

At the same time, it is known that the depth of the radiation penetration into the tissue in wIRA treatment is much less than the radius of the irradiated area on the body surface. This means that the axial radiative flux component is much greater that the radial component of the radiative flux. Therefore, it seems reasonable to neglect radiative transfer in the tissues along the body surface in the computational model. It was shown in [10] that this assumption is acceptable. Such a 1-D approach is expected to decrease slightly the radiative power absorbed at the periphery of the irradiated region. In addition, the following special features of the problem make possible the use of 1-D approach to solve the problem under consideration:

- The incidence angles in the center of the irradiated surface of the body are small and the near-to-normal incidence is predominant in this region;
- The range of the incidence angles at the periphery of the irradiated region is also small and all the rays have approximately the same direction as the ray coming from the center of the lamp.

The linearity of the radiative transfer problem allows the use of the additive rule in analysis of the effect of angular distribution of the incident radiation at every point of the body surface. Therefore, a variation of the incidence angle in the calculations is sufficient to estimate the effect of non-collimated radiation.

The radiative transfer model suggested in this paper is based on the following additional assumptions:

- The radial transfer of radiation in a highly scattering human tissues is relatively small as compared with the radiative transfer in the axial direction;
- The effect of final size of the light source can be neglected, and one can independently consider a collimated oblique irradiation of the body surface at each of thin concentric layers of the computational region (the normal incidence takes place at the axis of symmetry only).

The latter means that the modified two-flux approximation [25] employed in papers [8,10] should be generalized for the case of

Table 1
Summary of skin sample characteristics from various research papers.

	Marchesini et al. [17]	Chan et al. [18]	Simpson et al. [19]	Troy et al. [20]	Bashkatov et al. [21]	Salomatina et al. [22]
Skin sample	In vitro	In vitro	Ex vivo	In vitro	In vitro	In vitro
Skin color	Caucasian	Caucasian	Caucasian	N/A	N/A	Caucasian
Epidermis thickness, mm	0.073 ± 0.024	0.42–0.5	1.5–2	2	0.1	0.06–0.1
Dermis thickness, mm	N/A				1–4	0.1–0.78
Fat layer thickness, mm	N/A	N/A	2	N/A	1–6	0.28–0.8
Skin locations	Upper leg, lower back, breast, thigh, abdomen, groin	Buttocks and hind leg	Abdominal, breast tissue	Knee, Lower back, shin, thigh, groin, scalp, facial tissue, abdomen	Peritoneum area (abdominal region)	Face, scalp, neck, back
Skin layers	Epidermis	Epidermis and partial dermis (combined)	Dermis, fat, muscle (separate)	Stratum corneum, epidermis, dermis (combined)	Fat layer	Epidermis, dermis, fat (separate)
Index of refraction	1.45	N/A	1.4	1.365	1.455	1.4

oblique incidence as it was done for particular case of a nonrefracting medium in paper [26]. Note that the modified two-flux approximation is based on approximate presentation of the angular dependence of radiation intensity in the form of a stepwise function with two constant but different values of the radiation intensity in some parts of the backward and forward hemispheres taking into account the effect of total internal reflection at the interfaces. In the case of oblique incidence, the radiation field in the body is three-dimensional. But it is clear that the profile of the absorbed radiation power is the same in the case of an axisymmetric illumination of the body by the rays propagating along the conical surface of the same angle. This feature of the radiative transfer has been already used by Dombrovsky et al. [26] to obtain the correct 1-D solution at oblique incidence.

Following [8–11] we use the transport approximation for the scattering phase function [24,27] when the scalar radiative transfer equation (RTE) for an isotropic medium can be written as follows [24,28,29]:

$$\vec{\Omega}\nabla I_\lambda\left(\vec{r},\vec{\Omega}\right)+\beta_\lambda^{\mathrm{tr}} I_\lambda\left(\vec{r},\vec{\Omega}\right)=\frac{\sigma_\lambda^{\mathrm{tr}}}{4\pi}\int_{(4\pi)} I_\lambda\left(\vec{r},\vec{\Omega}'\right)d\vec{\Omega}' \tag{2}$$

where $I_\lambda\left(\vec{r},\vec{\Omega}\right)$ is the spectral radiation intensity at point $\vec{r}$ in direction $\vec{\Omega}$, $\sigma_\lambda^{\mathrm{tr}}=\sigma_\lambda\cdot(1-\bar{\mu}_\lambda)$ is the transport scattering coefficient (σ_λ is the ordinary scattering coefficient, $\bar{\mu}_\lambda$ is the asymmetry factor of scattering), $\beta_\lambda^{\mathrm{tr}}=\alpha_\lambda+\sigma_\lambda^{\mathrm{tr}}$ is the transport extinction coefficient, α_λ is the absorption coefficient. Note that transport approximation has been widely used in radiative transfer calculations for many years. It was confirmed that the hemispherical characteristics of radiation field in scattering materials are well described using this approximation [24,27].

Let us consider the 1-D model problem when a plane-parallel layer of the medium is illuminated by a collimated radiation at a known angle with respect to the normal direction. The schematic of the particular example problem in which the layer is illuminated from one side by a monochromatic radiation is presented in Fig. 1. The geometrical parameters of this simplified picture can be taken from paper [10]. Using the optical properties of human tissues presented in Fig. 3, one can find that the spectral optical thickness of three superficial layers (epidermis, dermis and fat layers) is very large. Therefore, one can neglect reflection of the radiation from the interface between the fat and muscle layers. The latter simplifies the corresponding boundary condition. After integration over an azimuth angle, the RTE can be written as follows [24]:

$$\mu\frac{\partial I_\lambda}{\partial z}+\beta_\lambda^{\mathrm{tr}} I_\lambda=\frac{\sigma_\lambda^{\mathrm{tr}}}{2}\int_{-1}^{1} I_\lambda(z,\mu)d\mu \qquad \mu=\cos\theta \qquad 0<z<d \tag{3}$$

The boundary conditions at two surfaces of the layer are:

$$I_\lambda(0,\mu)=R_{\mathrm{f,int}} I_\lambda(0,-\mu)+\left(1-R_{\mathrm{f,ext}}\right)q_\lambda^{\mathrm{ext}}\delta(1-\mu_{\mathrm{int}})$$
$$\mu_{\mathrm{int}}=\sqrt{1-\left(1-\mu_{\mathrm{i}}^2\right)/n^2} \tag{4a}$$

$$I_\lambda(d,-\mu)=0 \qquad \mu>0 \tag{4b}$$

where $\mu_{\mathrm{i}}=\cos\theta_{\mathrm{i}}$, θ_{i} is the incidence angle, $\mu_{\mathrm{int}}=\cos\theta_{\mathrm{int}}$, θ_{int} is the angle of the reflected ray, $R_{\mathrm{f,int}}$ and $R_{\mathrm{f,ext}}$ are the Fresnel's reflectivities [29,30]. It will be clear from subsequent transformations that we do not need the general expressions for the reflectivities while using an approximate solution to the RTE. The following formulas for the reflectivities will be employed [29]:

$$R_{\mathrm{f,ext}}=\left(R_{\parallel,\mathrm{ext}}+R_{\perp,\mathrm{ext}}\right)/2 \tag{5a}$$

$$R_{\parallel,\mathrm{ext}}=\left(\frac{n^2\mu_{\mathrm{i}}-\sqrt{n^2-1+\mu_{\mathrm{i}}^2}}{n^2\mu_{\mathrm{i}}+\sqrt{n^2-1+\mu_{\mathrm{i}}^2}}\right)^2 \qquad R_{\perp,\mathrm{ext}}$$
$$=\left(\frac{\mu_{\mathrm{i}}-\sqrt{n^2-1+\mu_{\mathrm{i}}^2}}{\mu_{\mathrm{i}}+\sqrt{n^2-1+\mu_{\mathrm{i}}^2}}\right)^2 \tag{5b}$$

$$R_{\mathrm{f,int}}=\begin{cases}R_{\mathrm{f,n}} \text{ when } \mu>\mu_{\mathrm{cr}}\\ 1 \text{ when } \mu\leqslant\mu_{\mathrm{cr}}\end{cases} \quad R_{\mathrm{f,n}}=(n_{\mathrm{t}}-1)^2/(n_{\mathrm{t}}+1)^2 \quad \mu_{\mathrm{cr}}=\sqrt{1-1/n^2} \tag{6}$$

Eqs. (5) refer to the external collimated radiation, whereas approximate Eq. (6) will be used for the radiation coming to the body surface from inside. The above relations are not general but they are correct for the real case of biological tissues when the tissue index of absorption is relatively small: $\kappa\ll n$. The value of $R_{\mathrm{f,int}}=1$ for $\mu\leqslant\mu_{\mathrm{cr}}$ corresponds to the total internal reflection. Strictly speaking, the above equations are correct for ideally smooth interface only. Of course, this is not the case for the body surface but fortunately, this assumption is not important because the reflectance from semitransparent media is determined mainly by volumetric scattering [31,32].

Following the usual technique consider the radiation intensity I_λ as a sum of the diffuse component J_λ and the term which corresponds to the transmitted and reflected directional external radiation:

$$I_\lambda=J_\lambda+\left(1-R_{\mathrm{f\ ,ext}}\right)E_\lambda^{\mathrm{tr}}\delta(1-\mu_{\mathrm{i}})q_\lambda^{\mathrm{ext}} \tag{7}$$

where

$$E_\lambda^{\mathrm{tr}}=\exp\left(-\tau_\lambda^{\mathrm{tr}}/\mu_{\mathrm{i}}\right) \quad \tau_\lambda^{\mathrm{tr}}=\int_0^z\beta_\lambda^{\mathrm{tr}}dz \quad \tau_\lambda^{\mathrm{tr},0}=\int_0^d\beta_\lambda^{\mathrm{tr}}dz \tag{8}$$

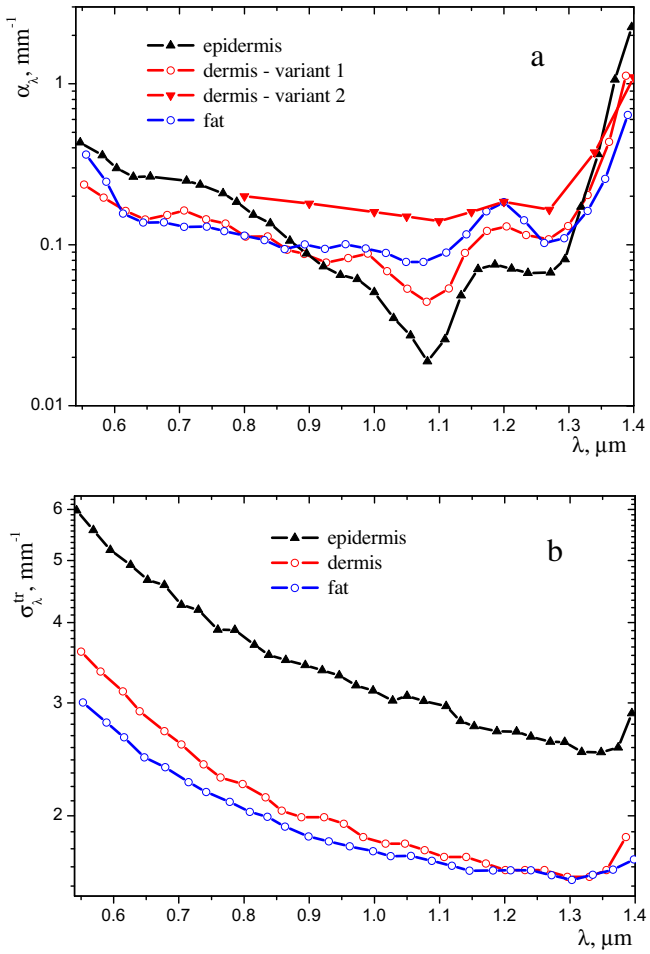

Fig. 3. Absorption coefficient (a) and transport scattering coefficient (b) of superficial human tissues. Epidermis: from [22]; Dermis: variant 1 and scattering coefficient – from [22], variant 2 – from [18]; Fat: from [22].

We used here the obvious relation $\delta(1-\mu_{int})=\delta(1-\mu_i)$.

The mathematical problem statement for the diffuse component of radiation intensity is as follows:

$$\mu\frac{\partial J_\lambda}{\partial z}+\beta_\lambda^{tr}J_\lambda=\frac{\sigma_\lambda^{tr}}{2}(G_\lambda+F_\lambda)\quad G_\lambda=\int_{-1}^{1}J_\lambda d\mu\quad F_\lambda=(1-R_{f,ext})E_\lambda^{tr}q_\lambda^{ext} \tag{9a}$$

$$J(0,\mu)=R_{f,int}(\mu)J(0,-\mu)\qquad J(d,-\mu)=0\qquad \mu>0 \tag{9b}$$

The spectral and integral (over the spectrum) radiation power absorbed in the medium are expressed as:

$$w_\lambda=-\int_{-1}^{1}\frac{dI_\lambda}{dz}\mu d\mu=\alpha_\lambda(G_\lambda+F_\lambda)\quad W=\int_{\lambda_1}^{\lambda_2}w_\lambda d\lambda \tag{10}$$

The above formulated problem for the diffuse component of the radiation intensity is still very complex. To simplify this problem one can use simple analytical representations of the angular dependence of the radiation intensity. It is known that the latter leads to the so-called differential approximations [24,27]. According to [10], the modified two-flux approximation is employed in the present paper. This approach is based on the following model for the angular dependence of radiation intensity [25]:

$$J_\lambda(z,\mu)=\begin{cases}J_\lambda^-(z), & -1\leqslant\mu<-\mu_{cr}\\ J_\lambda^0(z), & -\mu_{cr}<\mu<\mu_{cr}\\ J_\lambda^+(z), & \mu_{cr}<\mu\leqslant 1\end{cases} \tag{11}$$

Note that the case $\mu_{cr}=0$ corresponds to the ordinary two-flux model. The intermediate angle interval $-\mu_{cr}<\mu<\mu_{cr}$ gives no contribution to the radiation flux and the words "two-flux" are also applicable to the modified approximation. Integrating Eq. (7) separately over the intervals $-1<\mu<-\mu_{cr}$, $-\mu_{cr}<\mu<\mu_{cr}$, and $\mu_{cr}<\mu<1$, after simple transformations, one can obtain the following boundary-value problem for the function $g_\lambda=J_\lambda^-+J_\lambda^+$:

$$-\frac{d}{dz}\left(D_\lambda\frac{dg_\lambda}{dz}\right)+\frac{\alpha_\lambda}{1-\omega_\lambda^{tr}\mu_{cr}}g_\lambda=\frac{\sigma_\lambda^{tr}}{1-\omega_\lambda^{tr}\mu_{cr}}F_\lambda \tag{12a}$$

$$z=0,\quad D_\lambda\frac{dg_\lambda}{dz}=\frac{\gamma}{2}(1+\mu_{cr})g_\lambda\qquad z=d,\quad\frac{dg_\lambda}{dz}=0 \tag{12b}$$

where

$$D_\lambda=\frac{(1+\mu_{cr})^2}{4\beta_\lambda^{tr}}\quad\omega_\lambda^{tr}=\frac{\sigma_\lambda^{tr}}{\beta_\lambda^{tr}}\quad\gamma=\frac{1-R_{f,n}}{1+R_{f,n}} \tag{12c}$$

For simplicity, the value of normal reflectivity $R_{f,n}$ is used in Eq. (12c) as was done in [25]. It is not quite correct, and more accurate solution should be based on averaging of the reflectance recommended in [33]. It was shown in [34] by comparison with the exact numerical solutions that this correction improves the results in the case of a strongly refracting medium but there is no need in this correction for the particular problem under consideration.

The absorbed radiation power can be calculated using Eq. (10) and the following relation between functions G_λ and g_λ:

$$G_\lambda=\frac{(1-\mu_{cr})g_\lambda+\omega_\lambda^{tr}\mu_{cr}F_\lambda}{1-\omega_\lambda^{tr}\mu_{cr}} \tag{13}$$

As a result, we obtain the following relations for the spectral and integral volumetric absorption of radiation:

$$w_\lambda=\alpha_\lambda\frac{(1-\mu_{cr})g_\lambda+F_\lambda}{1-\omega_\lambda^{tr}\mu_{cr}}\qquad W=\int_{\lambda_1}^{\lambda_2}w_\lambda d\lambda \tag{14}$$

Note that one can consider a simpler approach than that discussed above. This can be done by ignoring the oblique incidence of radiation at any point to the irradiated surface of the body assuming that $\mu_i\equiv 1$. A comparison of the results obtained at normal incidence with the computational results obtained at realistic dependence of $\mu_i(r)$ will be done in this study to estimate the effect of the oblique incidence.

According to scheme in Fig. 1, we use the following radial dependence of the incidence angle:

$$\mu_i=H/\sqrt{H^2+r^2} \tag{15}$$

where H is the distance from the light source to the body surface.

4. Transient energy equation for heat transfer in human tissues

Strictly speaking, the transient energy equation for heat transfer in human tissues should include the terms responsible for metabolic heat generation and volumetric heat transfer between the tissue and arterial blood flow. Moreover, one can consider a two temperature model with an additional equation for arterial blood temperature as it was done in paper [9] (see also [35,36]). However, as was shown in [9], the complete heat transfer model can be simplified in the case of superficial tissues of the body far from big arterial vessels, where the local heat transfer between tissues and arterial blood is relatively small. As a result, it is sufficient to solve the following transient energy equation:

$$\rho c\frac{\partial T}{\partial t}=\nabla(k\nabla T)+W \tag{16}$$

where $W(t,r)$ is the volumetric heat generation due to the absorbed radiation. In the case of axisymmetric heat transfer problem, the boundary conditions for Eq. (16) are as follows:

$$r = 0 \quad \frac{\partial T}{\partial r} = 0 \qquad r = R \quad \frac{\partial T}{\partial r} = 0 \tag{17a}$$

$$z = 0 \quad k\frac{\partial T}{\partial z} = h_1(T_{e,1} - T) \qquad z = L \quad k\frac{\partial T}{\partial z} = h_2(T_{e,2} - T) \tag{17b}$$

where $T_{e,1}$ and $T_{e,2}$ are the temperatures of the ambient air and of the internal part of the body, respectively. Note that the thickness of the computational region in the heat transfer problem, L, should be chosen greater than the value of d for the radiative transfer problem because the depth of heat propagation into the body during thermal treatment is expected to be greater than the depth of the radiation penetration. Therefore, the muscle layer is included in the computational region in heat transfer calculations.

The simplest initial condition for the body temperature is as follows:

$$T(0, z, r) = T_0 \tag{18}$$

where the function $T_0(z)$ is the solution of the steady-state conduction problem:

$$\frac{d}{dz}\left(k\frac{dT}{dz}\right) = 0 \tag{19a}$$

$$z = 0 \quad k\frac{dT}{dz} = h_1(T_{e,1} - T) \qquad z = L \quad k\frac{dT}{dz} = h_2(T_{e,2} - T) \tag{19b}$$

Note that diffusion of water towards the body surface may be important in the case of a very intense external heating [37]. This effect is neglected in the present paper because of relatively mild conditions of thermal treatment. Another thermal effect analyzed in [37] is the evaporation of water from the body surface. This effect may be considerable especially in the beginning of the treatment, but at this stage we preferred to include it in the uncertainty of the convective heat transfer coefficient.

5. Computational results for model problem

The same layers of superficial human tissues as those in papers [7–11] were considered. The calculated profiles of the absorbed radiation power along the beam axis for the two variants of absorption coefficient of dermis are presented in Fig. 4. One can see a typical exponential behavior of the absorbed power with the distance z from the irradiated body surface. A considerable part of the incident radiative flux is reflected from the body mainly due to volumetric scattering of the radiation by human tissue. The calculated spectral reflectance is presented in Fig. 5. Obviously, the maximum reflectance at a wavelength of about 1.1 μm corresponds to the maximum of transport albedo of epidermis and dermis (see Fig. 3). Note that the difference between the curves for two variants of the absorption coefficient can be considered as an upper estimate of the uncertainty of optical properties of dermis for the wIRA spectral range.

In the case of the simplest model of normal incidence, the linearity of the radiative transfer problem leads to the following simple relation for the absorbed radiation power:

$$W(z, r) = W(z, 0) \cdot f(r) \tag{20}$$

where $W(z, 0)$ is the absorbed power profile shown in Fig. 4 and $f(r)$ is the radial distribution of normal radiative flux at the body surface. A relation similar to Eq. (20) is also correct in the case when the radial variation of the incidence angle is taken into account. Radiative flux at the body surface was measured using a *Minilux* (Marx Electronics Berlin) radiometer with a 10 mm entrance window. However, it is convenient to use an analytical approximation of the measured function $f(r)$ in the calculations. In the case of $H = 340$ mm, the following approximation in the region of $r < R = 150$ mm was chosen as close to the measured profile of the radiative flux:

$$f(r) = \begin{cases} 1, & r \leqslant R/3 \\ 1 - (3r/R - 1)/2, & R/3 < r < R \end{cases} \tag{21}$$

The range of the incidence angle is not wide for the particular model problem under consideration. The minimum value of the cosine of this angle is as follows:

$$\mu_i = H/\sqrt{H^2 + R^2} \approx 0.915 \tag{22}$$

This means that the effect of oblique incidence is very small and is confirmed by direct numerical calculations for the first variant of absorption coefficient of dermis presented in Fig. 6.

The computational results for the transient temperature field in the body depend on the thermal properties of the skin layers as well as conditions of heat exchange between the human body and surrounding air. In [38], the convective heat transfer coefficients of the human body for different postures were found to be in the range of $1.8 < h_1 < 4\ \mathrm{W\,m^{-2}\,K^{-1}}$ depending on the difference between skin and air temperature. These results agreed with other studies such as [39]. In [40] the value of $h = 7\ \mathrm{W\,m^{-2}\,K^{-1}}$ was used for estimating skin burn injuries. In subsequent calculations, the following parameters of heat transfer are used (see also [11]):

$$T_{e,1} = 295\ \mathrm{K} \quad h_1 = 5\ \mathrm{W m^{-2}\,K^{-1}} \quad T_{e,2} = 310\ \mathrm{K} \quad h_2 = 50\ \mathrm{W m^{-2}\,K^{-1}} \tag{23}$$

Note that calculations at different values of h_1 showed that the variation of this parameter does not practically affect computational results.

On another hand, thermal conductivity is the most important property in governing the temperature change and therefore, the uncertainty in the measurements of thermal conductivity can significantly affect the accuracy of temperature predictions. In [40] from the study of the effects of change in subcutaneous fat and dermis thermal conductivity it was concluded that the effects of variation of dermis thermal conductivity appeared to be less significant when compared with the effects of different fat thermal conductivity. Numerical results showed that the increase in fat thermal conductivity causes a significant decrease in the temperature at the interface between the subcutaneous fat and the dermis layer, i.e., the temperature of the affected tissue becomes lower due to the increase of fat conductivity thus allowing better heat transfer. In [41] it was also suggested that the influence of subcutaneous fat for external heating evaluation should be considered. Thermal property measurements undertaken in [42] showed that subcutaneous fat has the thermal conductivity $k = 0.23\ \mathrm{W\,m^{-1}\,K^{-1}}$ while in [40] and [43] the values for the fat thermal conductivity was given as $0.16\ \mathrm{W\,m^{-1}\,K^{-1}}$ and for the dermis thermal conductivity $0.37\ \mathrm{W\,m^{-1}\,K^{-1}}$ compared with 0.185 and 0.445 used in papers [8,9]. Two variants with different values of thermal conductivity are used in the calculations presented below (see Table 2). The uncertainty in thermal conductivity of epidermis was neglected because of a very small thickness of this layer. Note that the ranges of possible values of thermal conductivity used in papers [37,44] for other tissues were slightly wider: from 0.37 to $0.52\ \mathrm{W\,m^{-1}\,K^{-1}}$ for dermis and from 0.16 to $0.21\ \mathrm{W\,m^{-1}\,K^{-1}}$ for the subcutaneous fat.

Before proceeding to the transient heat transfer calculation, the initial temperature field in the body was obtained by numerical solution of the 1-D boundary-value problem (19). The calculated initial temperature profile is presented in Fig. 7. Obviously, the

steady-state profiles are linear in each of the four layers of the computational region.

To avoid possible overheating of the body during the thermal treatment, the wIRA radiator is normally getting switched off and on according to the surface temperature measured by infrared camera in the spectral range of human tissue opacity. In the example problem, we consider the simplest case of constant power radiator which is switched off when the skin surface temperature in the center of the irradiated region reaches the value of $T_s = 43$ °C and switched on again at $T_s = 42$ °C.

The transient heat transfer problem (16)–(18) at step-wise time variations of the absorbed power was solved numerically using the implicit finite-difference method and rectangular mesh. According to the radiative transfer calculations shown in Fig. 4, it was assumed that $W(z, r) = 0$ at $d < z < L$. Numerical data for the temperatures in the superficial layer of thickness $L = 2d = 7$ mm are presented in Figs. 8–10. The uniform rectangular computational mesh with 100 intervals in both the radial and axial directions was used in these calculations. Additional calculations showed that 100 intervals in the axial direction are sufficient for accurate calculations. As to the radial direction, it will be shown below that the number of intervals is not so important for the numerical solution, but 100 intervals were used for the detailed presentation of the computational results.

The results for both the complete 2-D conduction problem and for the local 1-D heat conduction problems (by ignoring heat conduction in the radial direction) are presented in Fig. 8 for two different values of dermis and fat thermal conductivity (see Table 2). It is clear from this figure that heat conduction in the radial direction can be neglected in practical calculations. This is an important methodological result because the possibility of use of 1-D problem for heat transfer is a significant additional simplification of the computational model. The oscillations of the curves for the surface temperature at $t > 3.5$ min are explained by imposed condition $42 < T_s < 43$ °C at $r = z = 0$. Note that the time needed after switching on to get the full radiation power is about 1 s, and a similar time is needed when switching off to decrease radiation to zero. This time is very small as compared with a typical period of the temperature oscillations and can be neglected in the calculations. The period of these oscillations is approximately constant and equal to 38 s for both variants of thermal conductivity. The amplitude of temperature oscillations decreases sharply with the distance from the body surface and becomes very small at $z = 3.5$ mm. It is interesting to note that thermal field in the boundary layer next to the surface of the body becomes very

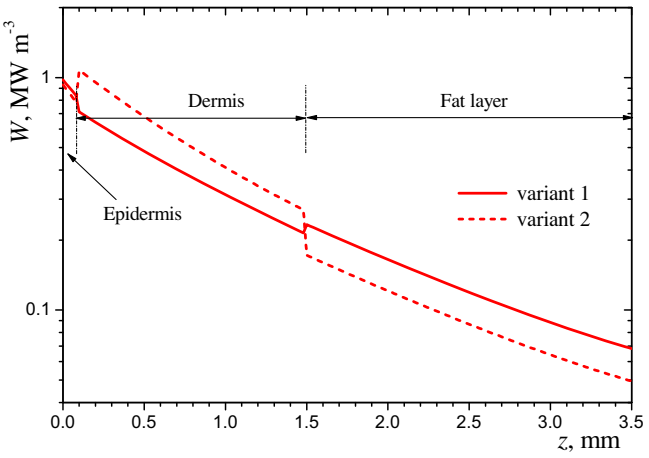

Fig. 4. Profile of absorbed radiation power along the beam axis: variants 1 and 2 see in Fig. 3.

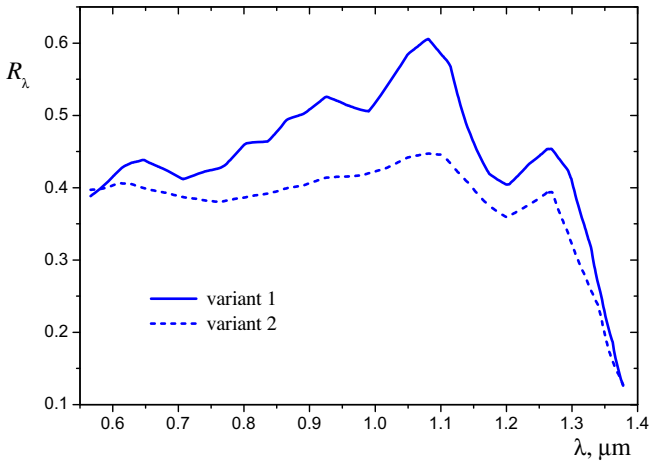

Fig. 5. Spectral hemispherical reflectance from the body surface: variants 1 and 2 see in Fig. 3.

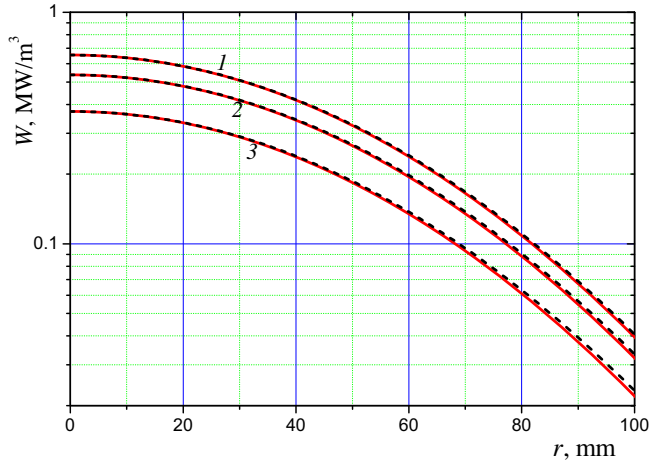

Fig. 6. Effect of oblique incidence on volumetric absorbed power of radiation at different distances from the body surface: 1 – $z = 0.35$ mm, 2 – $z = 0.7$ mm, 3 – $z = 1.4$ mm; Solid red curves – complete calculations, dashed black curves – locally normal incidence. (For interpretation of the references to color in this figure legend, the reader is referred to the web version of this article.)

close to the steady-state one after $t > 8$ min. The effect of changing dermis and fat thermal conductivity on the transient temperature profiles appears to be insignificant.

The effect of uncertainty in absorption coefficient of the dermis is illustrated in Fig. 9. The calculations showed that this effect is considerable only at the initial stage of body heating. The upper estimate of the absorption coefficient of the dermis (variant 2) also results in a decrease of the temperature oscillations period up to 30 s (instead of 38 s for variant 1). A comparison with the experimental data of [45] indicates that variant 1 is more realistic one. The computational results on the effect of absorption coefficient on the period of temperature oscillations are potentially interesting for determining the optical properties of human tissues using infrared diagnostics. This observation has been recently used to suggest a novel method to retrieve an average spectral absorption coefficient of superficial human tissues [46]. It is important to note that the steady-state thermal regime of the body is weakly sensitive to the uncertainty in the absorption coefficient of the dermis.

The axial temperature profiles at $t > 4$ min presented in Fig. 10 indicate almost uniform temperature in the layers of epidermis and dermis and a significant decrease in temperature at larger distance from the body surface. Of course, the temperature estimates

Table 2
Thermal properties of tissues in the computational region.

Layer number	Tissue name	ρc, MJ m^{-3} K^{-1}	k, W m^{-1} K^{-1} Variant 1/variant 2
1	Epidermis	4.31	0.235
2	Dermis	3.96	0.445/0.37
3	Fat	2.67	0.185/0.16
4	Muscle	4.12	0.51

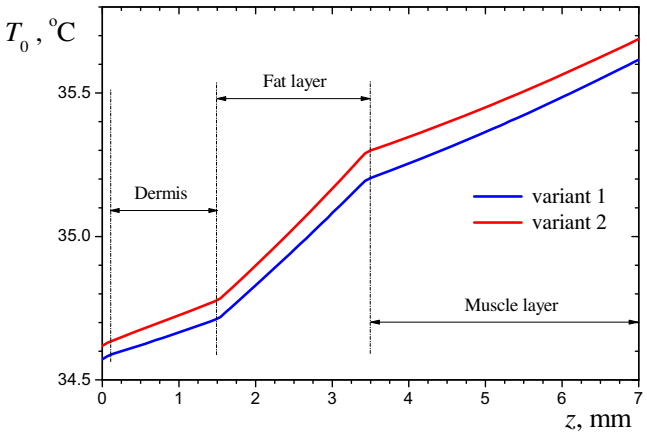

Fig. 7. Initial temperature profile in the body (before thermal treatment) for different variants of thermal conductivity.

in this part of the computational region are sensitive to the particular thermal conditions such as possible presence of bone or large blood vessels in the muscle layer. At the same time, one should note that calculated temperature profiles at $t \geqslant 8$ min indicate that the steady-state thermal regime of the body treatment is nearly reached before the onset of thermal regulation processes such as increased local blood flow.

The wIRA radiator *Hydrosun 750* was applied to achieve local hyperthermia in women with inoperable recurrent breast cancer in the area of chest wall [45]. To control the wIRA irradiation and to prevent heat overload and burns of the skin, the infrared measurements of the body surface temperature were made using a thermographic camera in the spectral range from 8 to 12 μm, and the spectral emissivity 0.98 of the surface was taken into account to retrieve the real temperature from these measurements. The overall resolution of the selected camera is estimated as ±0.4 °C. To evaluate the effect of this systematic error in temperature, additional calculations illustrated in Fig. 11 were performed. The resulting range of the oscillations period is from 36.9 to 39.4 s.

To make our computational model closer to the real conditions of thermal treatment, we should take into account the heating of the air layer between the hot lamp and the body surface. It means that the value of $T_{e,1}$ is not constant but increases with time. This time dependence can be described by the following exponential approximation:

$$T_{e,1} = T_{e,1}^{(1)} + \left(T_{e,1}^{(2)} - T_{e,1}^{(1)}\right)[1 - \exp(-t/t_h)] \quad (24)$$

where $T_{e,1}^{(1)} = 295$ K and the values of $T_{e,1}^{(2)}$ and t_h should be obtained from the experiment. An accurate determination of these parameters is beyond the scope of the present paper. Instead, a qualitative upper estimate with the following parameters is considered:

$$T_{e,1}^{(2)} = 315 \text{ K}, \quad t_h = 5 \text{ min} \quad (25)$$

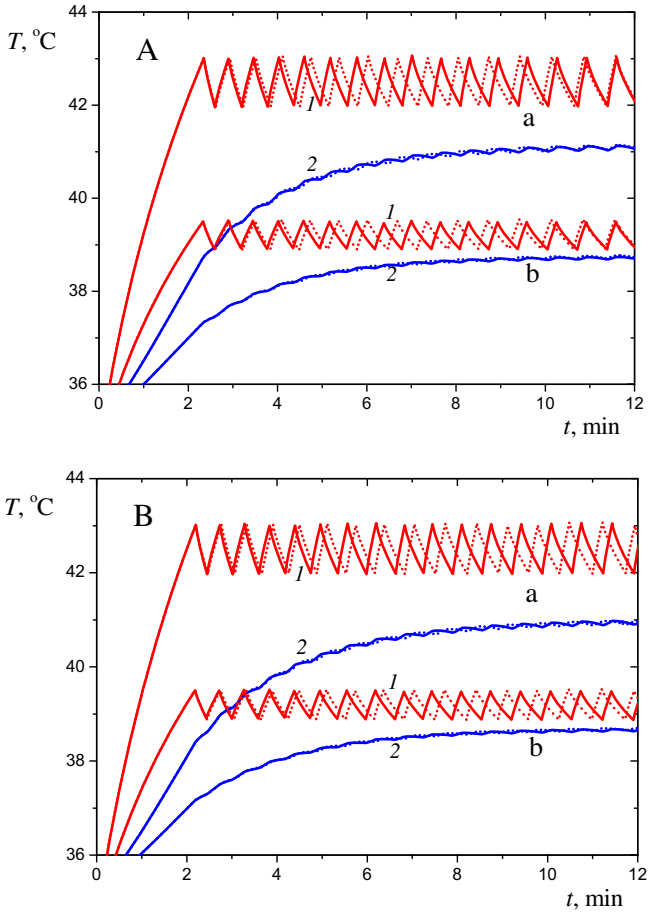

Fig. 8. Temperature variation (a) at the axis of the irradiated region and (b) at radius $r = 90$ mm: 1 – at the body surface, 2 – at distance $z = 3.5$ mm from the body surface. Calculations for different variants of thermal conductivity: A –variant 1, B – variant 2. Solid lines – 2-D heat conduction, dotted lines – 1-D heat conduction model. The first variant of dermis absorption coefficient was used in the calculations.

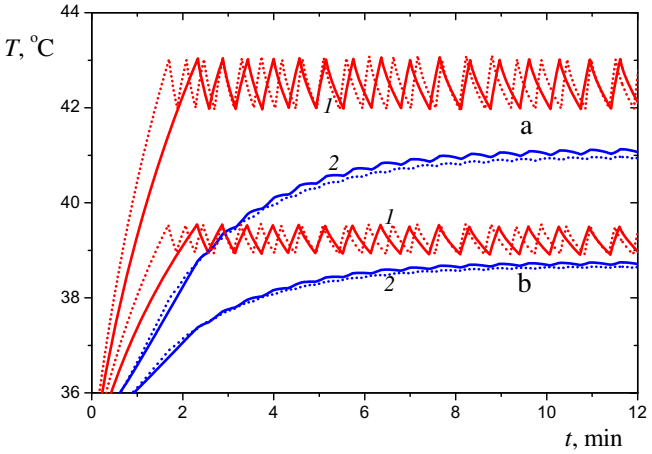

Fig. 9. Effect of the dermis absorption coefficient on temperature variation (a) at the axis of the irradiated region and (b) at radius $r = 90$ mm: 1 – at the body surface, 2 – at distance $z = 3.5$ mm from the body surface; Solid lines – variant 1 of absorption coefficient, dotted lines – variant 2. The 2-D approach and variant 1 of thermal conductivity were used in heat conduction calculations.

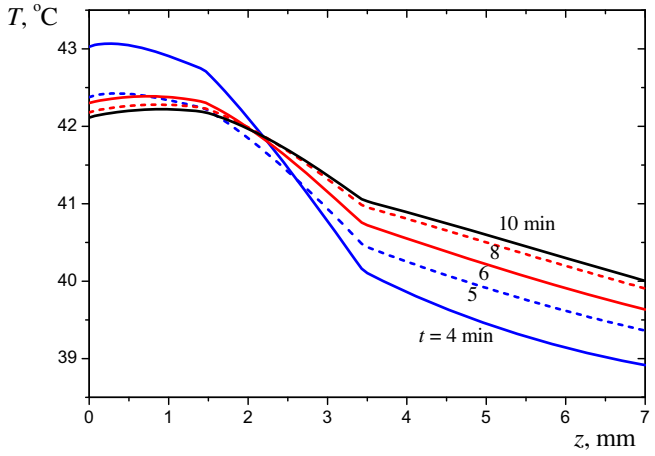

Fig. 10. Typical temperature profiles in the body at the axis of the incident beam.

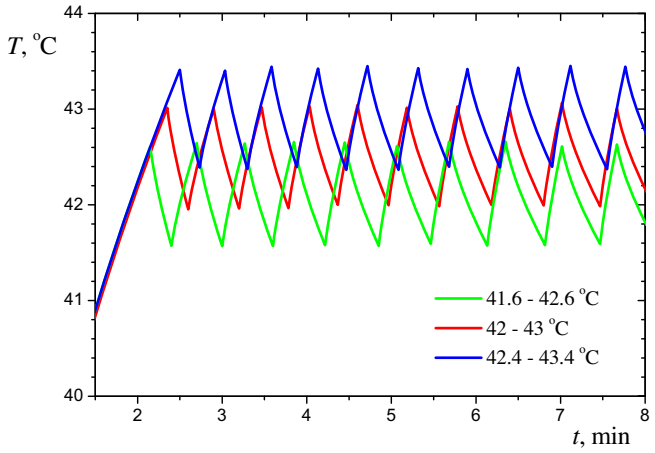

Fig. 11. The calculated variation of the body surface temperature at different ranges of this temperature; the 2-D calculations for variant 1 of thermal conductivity and variant 1 of absorption coefficient.

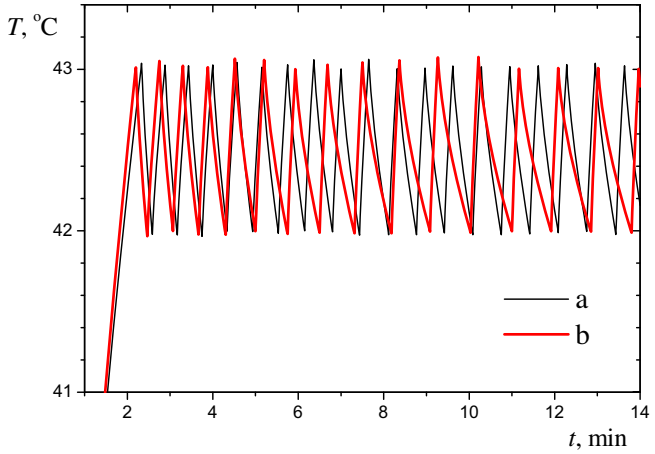

Fig. 12. Effect of air heating on time variation of the body surface temperature. The calculations (a) without air heating and (b) with air heating according to Eqs. (24) and (25). The variant 1 of thermal conductivity and variant 1 of absorption coefficient are considered.

One can see in Fig. 12 that a strong decrease in convective heat transfer with heating of air near the body surface results in an approximately two fold increase in the period of the surface temperature oscillations. This is in a good agreement with the experimental data obtained using the thermography based control system [45]. Note that conditions (25) lead to the results which are very close to the limiting case of negligible convective heat transfer when the oscillation period is controlled by the absorption coefficient and thermal conductivity of superficial tissues.

Note that parameters of the model developed can be corrected during the treatment on the basis of measurements of the temperature oscillation period. Of course, this is beyond the scope of the present paper.

6. Conclusions

A combined computational model for the transient thermal treatment of superficial human tissues using water-filtered infrared irradiation has been developed. The model includes solutions of both the spectral radiative transfer problem and the transient heat transfer problem for the case of a periodic irradiation. The period of this irradiation for the desirable range of the body surface temperature was computationally determined.

The computational analysis showed that both the radiative transfer and heat transfer by conduction in the body can be sufficiently accurately obtained using relatively simple 1-D models without time-consuming 2-D calculations.

The effect of uncertainty in spectral absorption coefficients on thermal treatment parameters was analyzed. It was shown that the temperature response to periodic infrared heating in combination with simultaneous measurements of the body surface temperature is a promising way to estimate the optical properties of superficial tissues. The effect of change of dermis and fat thermal conductivity, on other hand, appears to be insignificant for the chosen parameters.

A better agreement between the computational prediction for the periodic variation of the body surface temperature and the experimental results was observed when a heating of the air layer between the hot lamp and the body surface was taken into account. Further improvement of the model can be reached using an in situ correction of the skin optical and thermal parameters according to the thermal response of the patient skin.

Conflict of interest

None declared.

Acknowledgments

The first author is grateful for the partial financial support of this work by the University of New South Wales (Sydney) and Russian Foundation for Basic Research (Grant no. 13-08-00022a).

References

[1] T. Jung, T. Grune, Experimental basis for discriminating between thermal and athermal effects of water-filtered infrared A irradiation, Ann. N.Y. Acad. Sci. 1259 (2012) 33–38.
[2] G. Hoffmann, Principles and working mechanisms of water-filtered infrared-A (wIRA) in relation to wound healing, GMS Hyg. Infect. Control 2 (2) (2007) 1–15.
[3] D.K. Kelleher, O. Thews, J. Rzeznik, A. Scherz, Y. Salomon, P. Vaupel, Water-filtered infrared-A-radiation: a novel technique for localized hyperthermia in combination with bacteriochlorophyll-based photodynamic therapy, Int. J. Hyperthermia 15 (6) (1999) 467–474.
[4] M. Notter, H. Piazena, W. Müller, P. Vaupel, Low dose re-irradiation & thermography controlled wIRA hyperthermia in extended recurrent breast cancer, in: Proc. 31st Annual Meeting of the Society for Thermal Medicine, 6–10 May 2014, Minneapolis, MN, USA.

[5] H. Piazena, D.K. Kelleher, Effects of infrared-A irradiation on skin: discrepancies in published data highlight the need for an exact consideration of physical and photobiological laws and appropriate experimental settings, Photochem. Photobiol. 86 (3) (2010) 687–705.
[6] J. Vera, Y. Bayazitoglu, Gold nanoshell density variation with laser power for induced hyperthermia, Int. J. Heat Mass Transfer 52 (3–4) (2009) 564–573.
[7] J. Vera, Y. Bayazitoglu, A note on laser penetration in nanoshell deposited tissue, Int. J. Heat Mass Transfer 52 (13) (2009) 3402–3406.
[8] L.A. Dombrovsky, V. Timchenko, M. Jackson, G.H. Yeoh, A combined transient thermal model for laser hyperthermia of tumors with embedded gold nanoshells, Int. J. Heat Mass Transfer 54 (25–26) (2011) 5459–5469.
[9] L.A. Dombrovsky, V. Timchenko, M. Jackson, Indirect heating strategy of laser induced hyperthermia: an advanced thermal model, Int. J. Heat Mass Transfer 55 (17–18) (2012) 4688–4700.
[10] L.A. Dombrovsky, J.H. Randrianalisoa, W. Lipiński, V. Timchenko, Simplified approaches to radiative transfer simulations in laser induced hyperthermia of superficial tumors, Comput. Thermal Sci. 5 (6) (2013) 521–530.
[11] J.H. Randrianalisoa, L.A. Dombrovsky, W. Lipiński, V. Timchenko, Effects of short-pulsed laser radiation on transient heating of superficial human tissues, Int. J. Heat Mass Transfer 78 (2014) 488–497.
[12] F.A. Duck, Physical Properties of Tissue: A Comprehensive Reference Book, Acad. Press, San Diego, 1990.
[13] W. Cheong, S.A. Prahl, A.J. Welsh, A review of the optical properties of biological tissues, IEEE J. Quantum Electron. 26 (12) (1990) 2166–2185.
[14] J. Mobley, T. Vo-Dinh, Optical properties of tissue, in: T. Vo-Dinh (Ed.), Biomedical Photonics Handbook, CRC Press, Boca Raton (FL), 2003, pp. 2-1–2-75.
[15] V.V. Tuchin, Tissue Optics: Light Scattering Methods and Instruments for Medical Diagnosis, second ed., SPIE Press, Bellingham, WA, 2007. vol. PM166.
[16] S.L. Jacques, Optical properties of biological tissues: a review, Phys. Med. Biol. 58 (11) (2013) R37–R61.
[17] R. Marchesini, C. Clemente, E. Pignoli, M. Brambilla, Optical properties of *in vitro* epidermis and their possible relationship with optical properties of *in vivo* skin, J. Photochem. Photobiol., B 16 (2) (1992) 127–140.
[18] E.K. Chan, B. Sorg, D. Protsenko, M. O'Neil, A.J. Welch, Effect of compression on soft tissue optical properties, IEEE J. Sel. Top. Quant. Electron. 2 (4) (1996) 943–950.
[19] C.R. Simpson, M. Kohl, M. Essenpreis, M. Cope, Near-infrared optical properties of *ex vivo* human skin and subcutaneous tissues measured using the Monte Carlo inversion technique, Phys. Med. Biol. 43 (9) (1998) 2465–2478.
[20] T.L. Troy, S.N. Thennadil, Optical properties of human skin in the near infrared wavelength range of 1000 to 2200 nm, J. Biomed. Opt. 6 (2) (2001) 167–176.
[21] A.N. Bashkatov, E.A. Genina, V.I. Kochubey, V.V. Tuchin, Optical properties of human skin, subcutaneous and mucous tissues in the wavelength range from 400 to 2000 nm, J. Phys. D Appl. Phys. 38 (15) (2005) 2543–2555.
[22] E. Salomatina, B. Jiang, J. Novak, A.N. Yaroslavsky, Optical properties of normal and cancerous human skin in the visible and near-infrared spectral range, J. Biomed. Opt. 11 (6) (2006). paper 064026.
[23] A.N. Bashkatov, E.A. Genina, V.V. Tuchin, Optical properties of skin, subcutaneous and muscle tissues: a review, J. Innov. Opt. Health Sci. 4 (1) (2011) 9–38.
[24] L.A. Dombrovsky, D. Baillis, Thermal Radiation in Disperse Systems: An Engineering Approach, Begell House, New York, 2010.
[25] L. Dombrovsky, J. Randrianalisoa, D. Baillis, Modified two-flux approximation for identification of radiative properties of absorbing and scattering media from directional-hemispherical measurements, J. Opt. Soc. Am. A: 23 (1) (2006) 91–98.
[26] L.A. Dombrovsky, V.P. Solovjov, B.W. Webb, Attenuation of solar radiation by water mist and sprays from the ultraviolet to the infrared range, J. Quant. Spectrosc. Radiat. Transfer 112 (7) (2011) 1182–1190.
[27] L.A. Dombrovsky, The use of transport approximation and diffusion-based models in radiative transfer calculations, Comput. Thermal Sci. 4 (4) (2012) 297–315.
[28] J.R. Howell, R. Siegel, M.P. Mengüç, Thermal Radiation Heat Transfer, CRC Press, New York, 2010.
[29] M.F. Modest, Radiative Heat Transfer, third ed., Academic Press, New York, 2013.
[30] M. Born, E. Wolf, Principles of Optics, seventh (expanded) ed., Cambridge Univ. Press, New York, 1999.
[31] L.A. Dombrovsky, K. Ganesan, W. Lipiński, Combined two-flux approximation and Monte Carlo model for identification of radiative properties of highly scattering dispersed materials, Comput. Thermal Sci. 4 (4) (2012) 365–378.
[32] K. Ganesan, L.A. Dombrovsky, W. Lipiński, Visible and near-infrared optical properties of ceria ceramics, Infrared Phys. Tech. 57 (2013) 101–109.
[33] R. Siegel, C.M. Spuckler, Approximate solution methods for spectral radiative transfer in high refractive index layers, Int. J. Heat Mass Transfer 37 (Suppl. 1) (1994) 403–413.
[34] L.A. Dombrovsky, J.H. Randrianalisoa, W. Lipiński, D. Baillis, Approximate analytical solution to normal emittance of semi-transparent layer of an absorbing, scattering, and refracting medium, J. Quant. Spectrosc. Radiat. Transfer 112 (12) (2011) 1987–1994.
[35] A.-R.A. Khaled, K. Vafai, The role of porous media in modeling flow and heat transfer in biological tissues, Int. J. Heat Mass Transfer 46 (26) (2003) 4989–5003.
[36] A. Nakayama, F. Kuwahara, A general bioheat transfer model based on the theory of porous media, Int. J. Heat Mass Transfer 51 (11–12) (2008) 3190–3199.
[37] M. Fu, W. Weng, H. Yuan, Numerical simulation of the effects of blood perfusion, water diffusion, and vaporization on the skin temperature and burn injuries, Numer. Heat Transfer 65 (12) (2014) 1187–1203.
[38] Y. Kurazumi, T. Tsuchikawa, J. Ishii, K. Fukagawa, Y. Yamato, N. Matsubara, Radiative and convective heat transfer coefficients of the human body in natural convection, Build. Environ. 43 (12) (2008) 2142–2153.
[39] H. Ishigaki, T. Horikoshi, T. Uematsu, M. Sahashi, T. Tsuchikawa, T. Mochida, T. Hieda, N. Isoda, H. Kubo, Experimental study on convective heat transfer coefficient of the human body, J. Thermal Biol. 18 (5–6) (1993) 455–458.
[40] E.Y.K. Ng, H.M. Tan, E.H. Ooi, Boundary element method with bioheat equation for skin burn injury, Burns 35 (7) (2009) 987–997.
[41] L.I. Petrella, L.E. Maggi, R.M. Souza, A.V. Alvarenga, R.P.B. Costa-Félix, Influence of subcutaneous fat in surface heating of ultrasonic diagnostic transducers, Ultrasonics 54 (6) (2014) 1476–1479.
[42] M.A. El-Brawany, D.K. Nassiri, G. Terhaar, A. Shaw, I. Rivens, K. Lozhken, Measurement of thermal and ultrasonic properties of some biological tissues, J. Med. Eng. Technol. 33 (3) (2009) 249–256.
[43] E.Y.K. Ng, H.M. Tan, E.H. Ooi, Prediction and parametric analysis of thermal profiles within heated human skin using the boundary element method, Philos. Trans. R. Soc. A 368 (2010) 655–678.
[44] M. Gašperin, D. Juričić, The uncertainty in burn prediction as a result of variable skin parameters: an experimental evaluation of burn protective outfits, Burns 35 (7) (2009) 970–982.
[45] M. Notter, J.-F. Germond, E. Wolf, R. Berz, J.P. Berz, Thermography guided irradiation using water-filtered infrared-A (wIRA) and radiotherapy on recurrent breast cancer – First experiences and temperature analysis, Thermol. Int. 21 (2) (2011) 45–52.
[46] L.A. Dombrovsky, A novel method to retrieve spectral absorption coefficient of highly scattering and weakly absorbing materials, in: Proc. Eurotherm Seminar 105 "Computational Thermal Radiation in Participating Media V" (CTRPM V), 1–3 April 2015, Albi, France.